Journal of Photochemistry and Photobiology A: Chemistry 225 (2011) 36–41

Contents lists available at SciVerse ScienceDirect

Journal of Photochemistry and Photobiology A: Chemistry

journal homepage: www.elsevier.com/locate/jphotochem

Porous Photocatalytic Membrane Microreactor (P2M2): A new reactor concept for photochemistry

H.C. Aran[a], D. Salamon[b], T. Rijnaarts[a], G. Mul[c], M. Wessling[b], R.G.H. Lammertink[a,*]

[a] Soft Matter, Fluidics and Interfaces, MESA+, Faculty of Science and Technology, University of Twente, P.O. Box 217, 7500AE Enschede, The Netherlands
[b] Membrane Technology Group, MESA+, Faculty of Science and Technology, University of Twente, P.O. Box 217, 7500AE Enschede, The Netherlands
[c] Photocatalytic Synthesis, Faculty of Science and Technology, University of Twente, P.O. Box 217, 7500AE Enschede, The Netherlands

ARTICLE INFO

Article history:
Received 25 May 2011
Received in revised form
14 September 2011
Accepted 24 September 2011
Available online 1 October 2011

Keywords:
Photocatalysis
Microreactor
Membrane reactor
Surface modification
Methylene blue
Phenol
Oxygen

ABSTRACT

In this study, a new membrane microreactor concept for multiphase photocatalytic reactions is demonstrated. Microfabrication, photocatalyst immobilization and surface modification steps were performed to develop a Porous Photocatalytic Membrane Microreactor (P2M2). This concept benefits from a stable gas–liquid–solid (G–L–S) interface allowing a continuous supply of gaseous reactants and a reduced light path. A surface modification technique was devised to alter the wetting conditions of the reactor wall. Through a complete hydrophobization and a selective hydrophilization step by use of UV-light, we obtained a hydrophobic porous membrane support with hydrophilic photocatalytic microchannels. The photocatalytic degradations of methylene blue and phenol were used as model reactions to test the device, demonstrating promising degradation performance. We further demonstrated the effect of additional oxygen supply to the performance of the reactor for both reaction systems.

1. Introduction

Microreactors provide high surface to volume ratio, which leads to enhanced heat and mass transfer in these devices. Additionally, due to their miniaturized dimensions they facilitate safer operations, occupy small space and create less waste. These properties make them superior for many applications (e.g. in heterogeneous catalysis) and open new routes for chemical technology [1–6].

In recent years, microreactors also became attractive for photochemistry and photocatalytic processes [7–10]. Their high surface to volume ratio reduces mass transfer limitations, such that they overcome the setback of the low surface area of the immobilized macroscale wall reactors for photocatalysis [9,11]. Moreover, the miniaturized dimensions in the microreactors provide a reduced path for the light decreasing photon transfer limitations and lead to high illumination homogeneity along the reactor [7,9].

Many of the already existing concepts from microreaction technology have been adapted for photochemical and photocatalytic gas–liquid (G–L) and gas–liquid–solid (G–L–S) reactions. A remarkable reactor design for these purposes is the commercially available falling film microreactors utilized in G–L reactions [7]. In these reactors, a thin falling liquid film flows by gravitational force along a microstructured surface while it is illuminated by UV light and exposed to the co-flowing gas. Jähnisch et al. [12,13] applied falling film microreactors for photooxidation and photochlorination reactions, in which the liquid reactant was saturated with the gaseous reactant in this continuous manner. These reactors are well-suited for G–L photochemical reactions. However, for photocatalytic G–L–S reactions these reactors can suffer from mass transfer limitations, as the gas has to diffuse through the liquid film to reach an immobilized solid catalyst on the microstructured surface.

Another possible microreactor type for the application of photocatalysis is the dispersed phase microreactors. In these reactors the gaseous reactant is dispersed in the liquid phase (e.g. slug flow, annular flow) flowing in the microchannel. The dispersed phase microreactors benefit from enhanced mixing (mass transfer) in the liquid slugs inside the microchannel [14,15]. Lindstrom et al. [15] integrated slug flow and Matsushita et al. [16,17] investigated annular flow in microreactors for photocatalytic model reactions and they showed significant improvement in the performance of their microreactors, compared to single phase operation. For applications in which long microchannels are required, dispersed phase

* Corresponding author. Tel.: +31 534894798; fax: +31 534892882.
E-mail address: r.g.h.lammertink@utwente.nl (R.G.H. Lammertink).

1010-6030/$ – see front matter © 2011 Elsevier B.V. All rights reserved.
doi:10.1016/j.jphotochem.2011.09.022

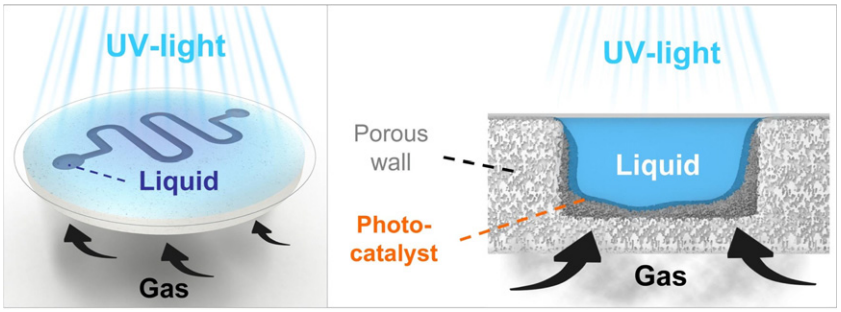

Fig. 1. Contacting concept of Porous Photocatalytic Membrane Microreactor (P2M2).

operation can result in depletion of gaseous reactants due to its consumption by the reaction [18]. In addition, the presence of gas bubbles in microchannels decreases the residence time of the liquid reactant in the reactor.

The aim of this study is to demonstrate a new concept for multiphase (G–L–S) photocatalytic reactions inside microreactors: Porous Photocatalytic Membrane Microreactor (P2M2). In this concept, the contacting of the G–L–S phases is established using membrane technology. The liquid flows inside microchannels (fabricated in porous aluminum oxide: α-Al_2O_3), where the photocatalyst (titanium dioxide: TiO_2) is immobilized on the channel wall (Fig. 1). The gas permeates through the porous wall of the membrane reaching the liquid that is flowing inside the microchannel. The microchannels are illuminated from the top by UV-light to stimulate the photocatalytic reaction.

This reactor design ensures that the liquid (L)–gas (G) interface is located at the solid (S) photocatalyst surface. We obtain this stable G–L–S interface by selective surface modification steps (hydrophobization and selective hydrophilization) of the intrinsically hydrophilic porous reactor materials. Photocatalytic degradations of methylene blue and phenol on TiO_2 catalyst were selected as model reactions in this work, in order to study the performance of the microreactor and the influence of oxygen (O_2) in these processes. The presence of O_2 is known to improve photocatalytic degradation of organic compounds [15,17,16,19]. The reactor concept presented in this study offers continuous supply of O_2 to the entire photocatalytic microreactor, avoiding its depletion due to consumption.

2. Experimental

2.1. Materials

Polyvinyl alcohol (PVA, Aldrich, Mowiol 8-88), MilliQ water, aluminum oxide (α-Al_2O_3; AKP-30, Sumitomo Chemical), nitric acid (HNO_3, Sigma–Aldrich, puriss, 65%) were used for the fabrication of the porous α-Al_2O_3 substrates. For the preparation of the photocatalyst coating, titanium dioxide (TiO_2, Evonik, Aeroxide P25, 99.5%), PVA (Aldrich, MW = 13,000–23,000 g/mol, 87–89%), acetic acid (Merck) and 2-propanol (Merck) were used. Perfluorinated octyltrichlorosilane (FOTS, Aldrich, 97%) and *n*-hexane (Merck) were used as received for the surface modification step. Methylene blue hydrate (MB; Fluka, purum p.a.) and phenol (Sigma–Aldrich) were used as model degradation compounds in this study.

2.2. Reactor preparation

The preparation of the Porous Photocatalytic Membrane Microreactor (P2M2) consists of five main stages (Fig. 2): (1) porous α-Al_2O_3 substrate fabrication, (2) microfabrication, (3) photocatalyst immobilization, (4) surface modification (a, complete hydrophobization; b, selective hydrophilization), and (5) module assembly.

(1) Porous α-Al_2O_3 substrates: These were prepared using an α-Al_2O_3 (AKP-30) suspension and colloidal filtration technique, as

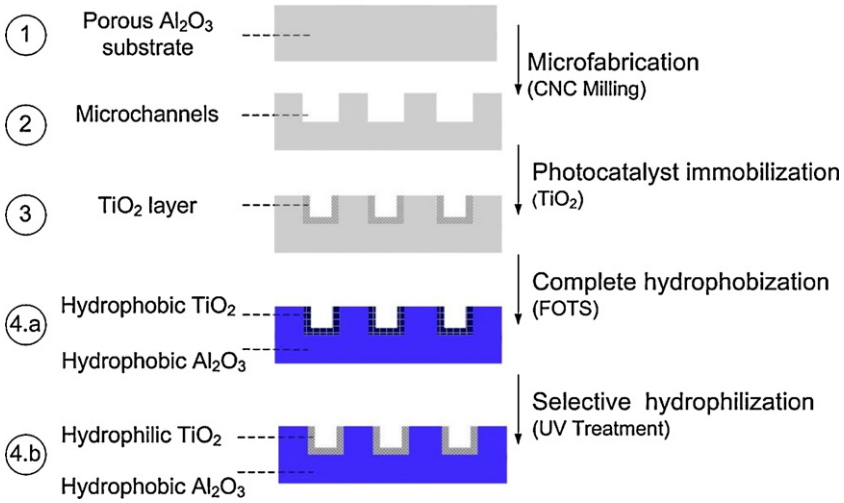

Fig. 2. Summary of P2M2 preparation steps: the illustrations represent the cross-section after each preparation step.

described elsewhere [20], resulting in circular supports with an average pore diameter of 80 nm and a porosity of 35%. After the sintering step (1100 °C), the substrates were cut and polished to reach a diameter of 39 mm and a thickness of 2 mm.

(2) Microfabrication: Substrates were fixed on a glass plate and 1 mm wide channels with a depth of 500 μm were milled in the flat α-Al_2O_3 substrates using a Sherline 5410 automated CNC-mill and a double cutter of 1 mm diameter. The channel length was 65 mm and the volume was ~32.5 μl.

(3) Photocatalyst immobilization: A TiO_2 suspension consisting of 1 g TiO_2, 1 g PVA, 50 ml 2-propanol and 50 ml H_2O was prepared. The pH was adjusted to ~2 by adding 5 g of acetic acid (CH_3COOH). The suspension was applied in the microchannels with a pipette. The excess suspension around the microchannels was wiped off with a tissue paper. The substrate was dried at 50 °C and sintered at 500 °C for 2 h. Subsequently, the substrate surface was polished to remove the excess TiO_2 outside the microchannels. The morphology of the immobilized TiO_2 catalyst was characterized by Scanning Electron Microscopy (SEM, JEOL TSM 5600). The BET surface area of the TiO_2 layer was measured using N_2-adsorption (Micromeritics Tristar).

(4) Surface modification For complete hydrophobization (α-Al_2O_3 and TiO_2), the samples were immersed in a solution containing 0.2 g of FOTS in 50 ml n-hexane. The substrate was kept in the solution for 1 h, taken out of the solution and then placed in an oven at 100 °C (adapted from previous work [3]). For selective hydrophilization of the TiO_2 photocatalyst layer, the completely hydrophobized sample was exposed to UV-light. The exposure time was varied in the order of minutes to determine optimum modification parameters. The surface properties (hydrophobicity) of the porous α-Al_2O_3 and TiO_2 were characterized by water contact angle measurements (OCA 15 Dataphysics) on each layer. The measurements were performed after the complete hydrophobization step and also after each UV-exposure time interval. The samples were rinsed with 2-propanol and then dried after each surface modification stage.

(5) Module assembly: The open microchannels on the substrate were covered with a UV-transparent foil (Hevel). The foil was softened on the top of the substrate with a heat treatment in the oven at 120 °C for 30 min. After cooling down, the foil attached to the surface of the substrate. Following that, the reactor was placed in an in-house built gas-tight module (PMMA, prepared by CNC Milling), which was connected to the light-guides of the UV-light source (Fig. 3).

2.3. Reactor operation

Aqueous solutions of methylene blue (~70 μM) and phenol (~1 mM) were prepared as liquid reactants. The liquid reactant solutions were pumped to the microreactor with flow rates of 10, 30 and 50 μl/min using a syringe pump (Harvard, Picoplus). Oxygen (O_2), air or nitrogen (N_2) was fed as gaseous reactant to the gas reservoir of the module (25 ml/min, atmospheric pressure).

The methylene blue (MB) concentration at the reactor inlet and outlet was determined by light absorbance measurements using an online UV–Vis Detector (Varian, Prostar 340) with a tungsten lamp (380–800 nm) at a fixed wavelength. The wavelength (λ) was set to 663 nm (maximum absorption of MB) and calibration was carried out for different concentrations of MB solution (from 10 to 100 μM).

The photocatalytic degradation of phenol and its products were characterized by analyzing the UV–vis spectrum of the reactor inlet and outlet. The reactor outlet was connected to a micro HPLC flow-through cell (ZEUTEC). The flow-through cell was attached to a deuterium halogen light source (DT-Mini-2-GS, Mikropack GmbH) and a high-resolution fiber optic spectrometer (HR4000, Ocean Optics Inc.) via two optical fibers (SR 600 nm, Ocean Optics Inc.), as described by Costantini et al. [21].

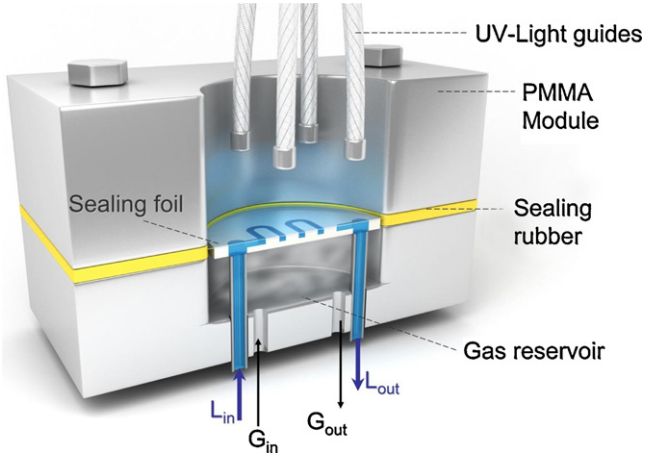

Fig. 3. Schematic representation of the fabricated PMMA reactor module (cross-sectional view).

As a light source for the photocatalytical reactions, a 120 W UV-lamp (HP-120, Dr. Gröbel UV-Elektronik GmbH) was used. The light was focused on the reactor using four light-guides. The average measured light intensity (Newport Optical Power Meter, 1916-C) at λ = 365 nm on the reactor surface was approximately 100 mW/cm^2.

3. Results and discussion

3.1. Reactor characterization

Fig. 4 shows a fabricated microchannel in porous α-Al_2O_3 substrate with the TiO_2 layer inside after the surface modification steps. It was observed that the inner walls of the microchannel were entirely covered with TiO_2 (Fig. 4b and c). The BET surface area of the TiO_2 layer was found to be approximately 45 m^2/g.

With the first surface modification using an FOTS coating (complete hydrophobization – Fig. 2a), the whole sample (α-Al_2O_3 and TiO_2) was successfully hydrophobized. The hydrophobicity of the sample was characterized by measuring the contact angle of a water droplet on the sample surface. The contact angles for both layers were around 150°, measured on porous α-Al_2O_3 and TiO_2 layers. The measured contact angle values were higher than what we have observed for a dense α-Al_2O_3 layer with FOTS coating (~115°) in our previous work [3]. Most likely, the surface roughness of the porous layers in this present study further enhances the hydrophobicity. Generally, if the contact angle on a flat and smooth surface (intrinsic contact angle of the surface) is greater than 90 °, roughening of this same surface will lead to a greater contact angle because of the enhanced liquid–solid interaction area [22].

The complete hydrophobization step efficiently ensures that the liquid does not wet the porous α-Al_2O_3 substrate. Nevertheless, it also hydrophobizes the TiO_2 layer in the microchannel. The hydrophobicity of the TiO_2 layer prevents an intensive contact between this photocatalyst layer and the liquid reactant, which would limit the reactor performance. Therefore, a selective hydrophilization step was carried out subsequently using of UV-irradiation. The change in the surface properties were characterized by measuring the water contact angle for both α-Al_2O_3 and TiO_2 layers after various intervals of UV-irradiation. We observed that after the irradiation the contact angle of α-Al_2O_3 remained constant, but of TiO_2 drastically decreased over time. After 1 h of UV-irradiation on the sample, the TiO_2 reached a contact angle of 0°.

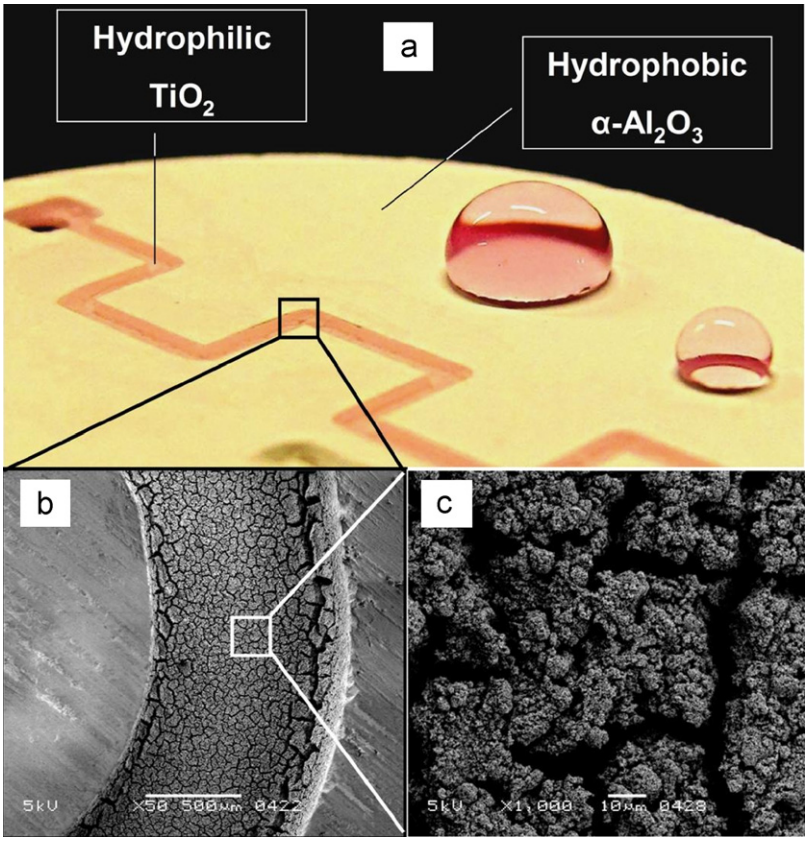

Fig. 4. Home-fabricated porous α-Al_2O_3 microreactor with immobilized TiO_2 and modified surface properties. (a) Visualization of the surface properties after the selective hydrophilization step, (b) and (c) SEM images of the ceramic membrane after photocatalyst immobilization: immobilized TiO_2 in the porous Al_2O_3 microchannel.

This method ensures a stable G–L–S interface in the microreactor on the porous α-Al_2O_3 hydrophobic membrane, while providing an intensive contact of the liquid reactant with the hydrophilic TiO_2 photocatalyst inside the microchannel (Fig. 4a).

The change in the surface properties of TiO_2 under light illumination was previously observed and investigated in literature [23–28]. This phenomenon attracted much attention; however the understanding of it is still under debate. One of the most widely accepted hypotheses explains it by the photocatalytic properties of the TiO_2 layer. With UV-illumination the hydrocarbons on the surface get photocatalytically decomposed by TiO_2 [26,27]. Another hypothesis is the structural change of the TiO_2 by formation of surface hydroxyl groups under UV-irradiation, which cause the switch to the hydrophilic state [23,25]. This hypothesis would be valid for TiO_2 films without an additional hydrocarbon coating. Regardless of the reason for this phenomenon, the presented method allows us to selectively tune the surface properties in the microchannel for a porous membrane reactor application in heterogeneous catalysis.

3.2. Reactor operation

The photocatalytic properties of the P2M2 were tested for the degradations of MB ($C_{16}H_{18}ClN_3S$) and phenol (C_6H_5OH) and showed promising degradation properties with additional O_2 supply through the porous membrane. The main performance criterion was degradation rate for both compounds. The presence of the UV-light, liquid reactant flow rate and the gas supply through the porous membrane were studied for these reactions.

3.2.1. Photocatalytic degradation of methylene blue

Fig. 5 displays the MB concentration of the outlet flow in time. At the initial stage of the experiment (1) without the presence of UV-light, MB adsorbs on the surface of the TiO_2 in the microchannel, which results in a lower MB concentration at the reactor outlet. After ~60 min, equilibrium was reached and the UV-light was exposed to the reactor (2). With the illumination the MB concentration at the reactor outlet decreases significantly due to the photocatalytic degradation. The decrease in the concentration indicated a MB degradation of ~27% (without additional O_2 supply). At the final stage (3), when the UV-light was turned off, the MB concentration increased and reached the initial concentration as in the initial stage of the experiment.

The degradation of MB was studied for different liquid flow rates: 10, 30 and 50 µl/min (residence times: 3.3, 0.7 and 0.3 min,

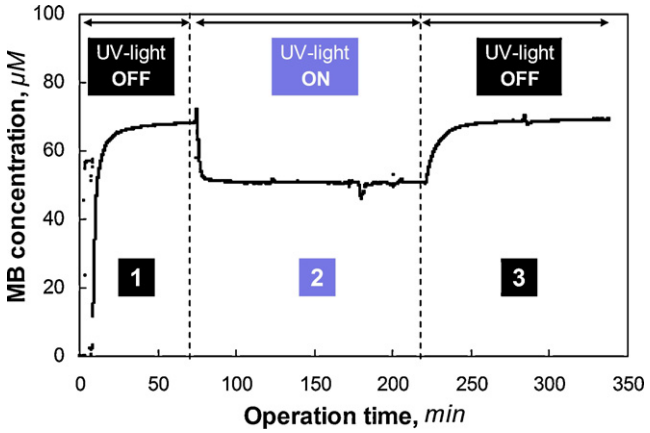

Fig. 5. Effect of UV-light on the MB degradation (initial MB concentration = 70 µM, liquid flow rate = 50 µl/min, without O_2 supply): MB concentrations are based on absorbance measurements of the reactor outlet at λ = 663 nm.

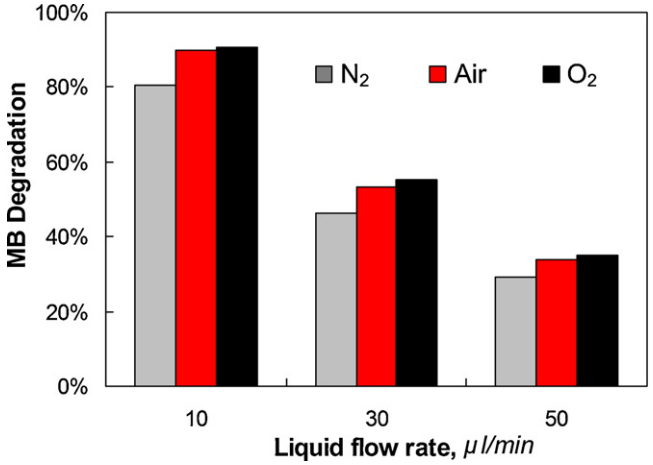

Fig. 6. Effect of O_2 supply and liquid flow rate on the MB degradation (initial MB concentration = 70 μM).

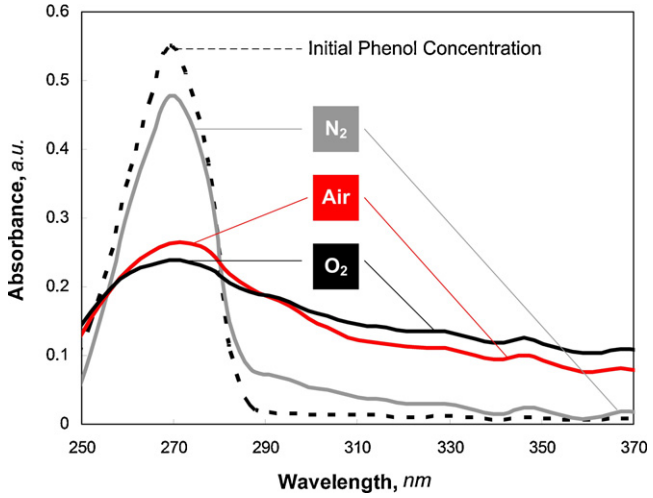

Fig. 7. Effect of O_2 supply on the photocatalytic phenol degradation (initial phenol concentration = 1 mM, liquid flow rate = 10 μl/min). Absorbance spectrum of the reactor inlet and outlet streams for different gas phase compositions.

respectively). As expected, the experiments showed that with increasing flow rate (10, 30 and 50 μl/min), the degradation of MB decreased (90%, 55% and 35% respectively – with O_2 supply) due to the decreasing residence time.

In order to determine the influence of membrane assisted O_2-supply in the MB degradation, tests with nitrogen (N_2), air and O_2 supply were performed. The conversion with air and pure O_2 supply were comparable (Fig. 6). The results showed that the conversion values with air and O_2 supply were slightly higher than with N_2.

O_2 is known to act as an electron acceptor in the photocatalytic degradation, forming superoxide radicals (O_2^-) as an oxidant. Furthermore, the presence of O_2 decreases recombination of the electron (e^-) and hole (h^+) pairs, which are generated by the photocatalyst. This also increases the efficiency of the formation of powerful oxidants such as hydroxyl radicals [15,29,30]. Nevertheless, as can be seen in Fig. 6, the additional supply of O_2 did not affect the degradation rate of methylene blue drastically. This can be explained by possible mass transfer limitations in the liquid phase or the low initial concentration (70 μM) of methylene blue, requiring only little amount of additional O_2. Apparently, for our configuration the hydroxyl radicals were formed fast enough by the UV-irradiation and the contribution of the superoxide free radicals was smaller.

Wu et al. [29] reported that the increase of dissolved O_2 concentration in the liquid reactant did not have an effect on the MB degradation rate in a batch slurry reactor. On the other hand, Lindstrom et al. [15] proved a significant positive effect of additional O_2 supply on the degradation of methylene blue in a microreactor. It must be noted that in the work of Lindstrom et al. [15] O_2 bubbles were dispersed in the liquid microchannel creating slug flow, which would also improve the mass transfer properties in this channel. In our reactor, the hydrodynamic properties in the microchannel were identical for the experiments with and without additional O_2 supply, so that merely the impact of O_2 in the reaction can be analyzed.

3.2.2. *Photocatalytic degradation of phenol*

In order to analyze the phenol degradation, the UV–vis absorbance of the inlet and outlet product were monitored online. The analysis of the absorbance was performed at wavelengths of $250 < \lambda < 400$ nm (Fig. 7).

The photocatalytic degradation of phenol was studied for different gas phase compositions. The additional O_2 supply increased the degradation of phenol drastically. As can be seen in Fig. 7 (initial phenol concentration = 1 mM, liquid flow rate= 10 μl/min), with O_2 supply (air or pure O_2), the absorbance peak of phenol at 270 nm decreased significantly compared to the values with N_2 supply.

The photocatalytic degradation of phenol was intensively studied as a model reaction in photocatalysis. It is a well-known fact that during phenol degradation, several aromatic intermediates are formed such as hydroquinone, benzoquinone and catechol. The formation of these intermediates was also observed in our reaction product, which is indicated by the increased absorbance at wavelengths higher than 290 nm (Fig. 7). Moreover, the product had a very light yellow/brown color, which is most likely due to the formation of reaction intermediates [31,19,32,33].

With increasing flow rate (decreasing residence time) the degradation of phenol decreased. Unfortunately, the decreasing peak of phenol cannot be related directly to the conversion value of phenol. The formed intermediate products (e.g. 1,4-benzoquinone, hydroquinone) also absorb around 270 nm.

Nevertheless, the measurements clearly show that the phenol degradation is improved with the membrane-assisted O_2 supply to the reaction zone. These results suggest that the utilization of membrane technology in photocatalytic processes is an attractive and promising alternative in multiphase systems.

4. Conclusions and outlook

A new microreactor concept for photocatalytic gas–liquid–solid (G–L–S) systems was introduced in this work. In contrast to the existing concepts, Porous Photocatalytic Membrane Microreactor (P2M2) exploits tuned interfaces to ensure a well-defined and stable G–L–S interface for the reaction and allows supplying the gaseous reactant continuously along the length of the microreactor. Microreactors with controlled surface properties and photocatalytic activity were successfully prepared by microfabrication, photocatalyst immobilization and selective surface modification steps.

We showed that the selective surface modification step ensures that the photocatalyst becomes hydrophilic precisely in photocatalytically active areas. This method can be applied for membrane reactors especially in heterogeneously catalyzed processes.

We also proved that the availability of the gaseous reactant O_2 in photocatalytic processes can be significantly improved by its continuous distribution to the reaction zone through a porous membrane. The presented results showed that the

membrane-assisted supply of O_2 enhanced the photocatalytic degradation of phenol and methylene blue.

Ongoing work in our research group is focused on numerical modeling of the presented degradation process for a better understanding of the mass transfer (diffusion), photon transfer (irradiation) and the reaction mechanisms (kinetics) that occur in photocatalytic processes.

Acknowledgements

This work was financially supported by Stichting voor de Technische Wetenschappen (STW, Project 07569) in Netherlands. We are grateful to J.G.F. Heeks, and J.A.M. Vrielink for technical support and analysis. The authors also greatly acknowledge J.M. Jani for the fruitful discussions and J. Bennink (Tingle.nl) for the illustrations.

References

[1] M.N. Kashid, L. Kiwi-Minsker, Microstructured reactors for multiphase reactions: state of the art, Industrial & Engineering Chemistry Research 48 (14) (2009) 6465–6485.
[2] V. Hessel, P. Angeli, A. Gavriilidis, H. Löwe, Gas–liquid and gas–liquid–solid microstructured reactors: contacting principles and applications, Industrial & Engineering Chemistry Research 44 (25) (2005) 9750–9769.
[3] H.C. Aran, J.K. Chinthaginjala, R. Groote, T. Roelofs, L. Lefferts, M. Wessling, R.G.H. Lammertink, Porous ceramic mesoreactors: A new approach for gas–liquid contacting in multiphase microreaction technology, Chemical Engineering Journal 169 (1–3) (2011) 239–246.
[4] A. Gavriilidis, P. Angeli, E. Cao, K.K. Yeong, Y.S.S. Wan, Technology and applications of microengineered reactors, Chemical Engineering Research and Design 80 (1) (2002) 3–30.
[5] K. Jähnisch, V. Hessel, H. Löwe, M. Baerns, Chemistry in microstructured reactors, Angewandte Chemie International Edition 43 (4) (2004) 406–446.
[6] H.C. Aran, S. Pacheco-Benito, M.W.J. Luiten-Olieman, S. Er, M. Wessling, L. Lefferts, N.E. Benes, R.G.H. Lammertink, Carbon nanofibers in catalytic membrane microreactors, Journal of Membrane Science 381 (1–2) (2011) 244–250.
[7] E.E. Coyle, M. Oelgemoller, Micro-photochemistry: photochemistry in microstructured reactors the new photochemistry of the future? Photochemical & Photobiological Sciences 7 (2008) 1313–1322.
[8] R. Gorges, S. Meyer, G. Kreisel, Photocatalysis in microreactors, Journal of Photochemistry and Photobiology A: Chemistry 167 (2–3) (2004) 95–99.
[9] T. van Gerven, G. Mul, J. Moulijn, A. Stankiewicz, A review of intensification of photocatalytic processes, Chemical Engineering and Processing 46 (9) (2007) 781–789.
[10] Y. Matsushita, N. Ohba, S. Kumada, K. Sakeda, T. Suzuki, T. Ichimura, Photocatalytic reactions in microreactors, Chemical Engineering Journal 135 (Suppl. 1) (2008) S303–S308.
[11] R. van Grieken, J. Marugán, C. Sordo, C. Pablos, Comparison of the photocatalytic disinfection of *E. coli* suspensions in slurry, wall and fixed-bed reactors, Catalysis Today 144 (1–2) (2009) 48–54.
[12] K. Jähnisch, U. Dingerdissen, Photochemical generation and [4+2]-cycloaddition of singlet oxygen in a falling-film micro reactor, Chemical Engineering & Technology 28 (4) (2005) 426–427.
[13] H. Ehrich, D. Linke, K. Morgenschweis, M. Baerns, K. Jähnisch, Application of microstructured reactor technology for the photochemical chlorination of alkylaromatics, CHIMIA International Journal for Chemistry 56 (7) (2002) 647–653.
[14] M.T. Kreutzer, F. Kapteijn, J.A. Moulijn, J.J. Heiszwolf, Multiphase monolith reactors: chemical reaction engineering of segmented flow in microchannels, Chemical Engineering Science 60 (22) (2005) 5895–5916.
[15] H. Lindstrom, R. Wootton, A. Iles, High surface area titania photocatalytic microfluidic reactors, AIChE Journal 53 (3) (2007) 695–702.
[16] Y. Matsushita, M. Iwasawa, T. Suzuki, T. Ichimura, Multiphase photocatalytic oxidation in a microreactor, Chemistry Letters 38 (8) (2009) 846–847.
[17] Y. Matsushita, M. Iwasawa, N. Ohba, S. Kumada, T. Suzuki, T. Ichimura, Photocatalytic oxidation and alkylation processes in microreactors, in: Nano/Micro Engineered and Molecular Systems, 2007. NEMS '07. 2nd IEEE International Conference on, 2007, pp. 851–854.
[18] A. Leclerc, M. Alame, D. Schweich, P. Pouteau, C. Delattre, C. de Bellefon, Gas–liquid selective oxidations with oxygen under explosive conditions in a micro-structured reactor, Lab Chip 8 (2008) 814–817.
[19] M. Subramanian, A. Kannan, Effect of dissolved oxygen concentration and light intensity on photocatalytic degradation of phenol, Korean Journal of Chemical Engineering 25 (2008) 1300–1308.
[20] A. Nijmeijer, H. Kruidhof, R. Bredesen, H. Verweij, Preparation and properties of hydrothermally stable α-alumina membranes, Journal of the American Ceramic Society 84 (1) (2001) 136–140.
[21] F. Costantini, W.P. Bula, R. Salvio, J. Huskens, H.J.G.E. Gardeniers, D.N. Reinhoudt, W. Verboom, Nanostructure based on polymer brushes for efficient heterogeneous catalysis in microreactors, Journal of the American Chemical Society 131 (5) (2009) 1650–1651.
[22] L. Cao, T.P. Price, M. Weiss, D. Gao, Super water- and oil-repellent surfaces on intrinsically hydrophilic and oleophilic porous silicon films, Langmuir 24 (5) (2008) 1640–1643.
[23] M. Miyauchi, N. Kieda, S. Hishita, T. Mitsuhashi, A. Nakajima, T. Watanabe, K. Hashimoto, Reversible wettability control of TiO_2 surface by light irradiation, Surface Science 511 (1-3) (2002) 401–407.
[24] Y.-H. Tseng, C.-S. Kuo, C.-H. Huang, T. Hirakawa, N. Negishi, H.-L. Bai, Photoinduced hydrophilicity of TiO_2 film as the effect of H_2O_2 addition, Micro Nano Letters, IET 5 (2) (2010) 81–84.
[25] M. Fernández-Rodríguez, V.J. Rico, A.R. González-Elipe, A. Álvarez-Herrero, Uv irradiation effects on TiO_2 thin films, Physica Status Solidi (c) 5 (5) (2008) 1164–1167.
[26] M. Takeuchi, K. Sakamoto, G. Martra, S. Coluccia, M. Anpo, Mechanism of photoinduced superhydrophilicity on the TiO_2 photocatalyst surface, The Journal of Physical Chemistry B 109 (32) (2005) 15422–15428.
[27] E. Balaur, J.M. Macak, L. Taveira, P. Schmuki, Tailoring the wettability of TiO_2 nanotube layers, Electrochemistry Communications 7 (10) (2005) 1066–1070.
[28] J. Wang, B. Mao, J.L. Gole, C. Burda, Visible-light-driven reversible and switchable hydrophobic to hydrophilic nitrogen-doped titania surfaces: correlation with photocatalysis, Nanoscale 2 (2010) 2257–2261.
[29] C.-H. Wu, J.-M. Chern, Kinetics of photocatalytic decomposition of methylene blue, Industrial & Engineering Chemistry Research 45 (19) (2006) 6450–6457.
[30] A. Houas, H. Lachheb, M. Ksibi, E. Elaloui, C. Guillard, J.-M. Herrmann, Photocatalytic degradation pathway of methylene blue in water, Applied Catalysis B: Environmental 31 (2) (2001) 145–157.
[31] S.K. Pardeshi, A.B. Patil, A simple route for photocatalytic degradation of phenol in aqueous zinc oxide suspension using solar energy, Solar Energy 82 (8) (2008) 700–705.
[32] Y.-T. Lin, C. Liang, J.-H. Chen, Feasibility study of ultraviolet activated persulfate oxidation of phenol, Chemosphere 82 (8) (2011) 1168–1172.
[33] B. Roig, C. Gonzalez, O. Thomas, Monitoring of phenol photodegradation by ultraviolet spectroscopy, Spectrochimica Acta Part A: Molecular and Biomolecular Spectroscopy 59 (5) (2003) 303–307.